[Supplementary material]

Engraved bones from the archaic hominin site of Lingjing, Henan Province

Zhanyang Li[1,2], Luc Doyon[1,3], Hao Li[4,5], Qiang Wang[1], Zhongqiang Zhang[1], Qingpo Zhao[1,2] & Francesco d'Errico[3,6,*]

[1] *Institute of Cultural Heritage, Shandong University, 27 Shanda Nanlu, Hongjialou District, Jinan 250100, China*

[2] *Henan Provincial Institute of Cultural Relics and Archaeology, 9 3rd Street North, LongHai Road, Guancheng District, Zhenzhou 450000, China*

[3] *Centre National de la Recherche Scientifique, UMR 5199—PACEA, Université de Bordeaux, Bât. B18, Allée Geoffroy Saint Hilaire, CS 50023, 33615 Pessac CEDEX, France*

[4] *Key Laboratory of Vertebrate Evolution and Human Origins, Institute of Vertebrate Paleontology and Paleoanthropology, Chinese Academy of Sciences, 142 Xizhimenwai Street, Xicheng District, Beijing 100044, China*

[5] *CAS Center for Excellence in Life and Paleoenvironment, 142 Xizhimenwai Street, Xicheng District, Beijing 100044, China*

[6] *SFF Centre for Early Sapiens Behaviour (SapienCE), University of Bergen, Øysteinsgate 3, Postboks 7805, 5020, Bergen, Norway*

[*] *Author for correspondence (Email: francesco.derrico@u-bordeaux.fr)*

OSM 1. Early engravings from Africa and Eurasia

Table S1. Early engravings from Europe, Asia and Africa (modified from Majkić *et al.* 2018a, 2018b).

Archaeological site	Country	Continent	Material	Cultural attribution	Age (kya)	Reference
Apollo 11	Namibia	Africa	Bone	MSA	71	(Vogelsang *et al.* 2010)
Blombos	South Africa	Africa	Ochre; Bone	MSA	100–75	(Henshilwood *et al.* 2002; 2009)
Border Cave	South Africa	Africa	Bone	ELSA	44–42	(d'Errico *et al.* 2012b; d'Errico *et al.* 2018)
Diepkloof	South Africa	Africa	OES	MSA	65–55	(Texier *et al.* 2010)
Klasies River	South Africa	Africa	Ochre	MSA	100–85	(d'Errico *et al.* 2012a)
Klein Kliphuis	South Africa	Africa	Ochre	MSA	80–50	(Mackay & Welz 2008)
Klipdrift Shelter	South Africa	Africa	OES	MSA	65–59	(Henshilwood *et al.* 2014)
Pinnacle Point	South Africa	Africa	Ochre	MSA	100	(Watts 2010)
Sibudu Cave	South Africa	Africa	Ochre; Bone	MSA	77–58; 56–29	(Cain 2004; Hodgskiss 2014)
Shuidonggou Loc. 1	China	Asia	Pebble	C&F	40	(Peng *et al.* 2012)
Xinglongdong	China	Asia	Tusk	C&F	120–150	(Gao *et al.* 2004)
Trinil	Indonesia	Asia	Shell	LP	540–430	(Joordens *et al.* 2015)
Mar-Tarik	Iran	Asia	Slab	MP-M	123	(Jaubert *et al.* 2009)
Qafzeh	Israel	Asia	Flint	MP-M	100	(Hovers *et al.* 1997)
Quneitra	Israel	Asia	Flint	MP-M	60	(d'Errico *et al.* 2003b; Goren-Inbar 1990)
Bacho Kiro	Bulgaria	Europe	Bone	MP-M	>47	(Bahn & Vertut 1997; Marshack 1976)
Kozarnika	Bulgaria	Europe	Bone	LP	900	(Sirakov *et al.* 2010)
Temnata Dupka	Bulgaria	Europe	Stone slab	MP	50	(Crémades *et al.* 1995)
Krapina	Croatia	Europe	Bone	MP	130	(Frayer *et al.* 2006)
Champlost Cave	France	Europe	Flint	MP-M	MIS3	(L'Homme & Normand 1993)
Chez Pourré-Chez Comte	France	Europe	Pebble	MP-M	MIS3	(L'Homme & Normand 1993)
Grotte du Renne	France	Europe	Bone	C	41–36	(d'Errico *et al.* 1998; d'Errico, *et al.* 2003a; Zilhão 2007)

Archaeological site	Country	Continent	Material	Cultural attribution	Age (kya)	Reference
La Chapelle Aux Saints	France	Europe	Bone	MP-LM	60	(d'Errico *et al.* 2009; Langley *et al.* 2008)
La Ferrassie	France	Europe	Bone	MP-M	65	(Capitan & Peyrony 1912; Zilhão 2007)
Le Moustier	France	Europe	Bone	MP-M	40	(Langley *et al.* 2008)
Marillac	France	Europe	Bone	MP-LM	46	(d'Errico *et al.* 1998; 2009, 2018; Maureille *et al.* 2010)
Roc de Combe	France	Europe	Bone	C	40	(d'Errico *et al.* 1998)
Roche au Loup	France	Europe	Bone	C	40	(d'Errico *et al.* 1998)
Terra Amata	France	Europe	Pebble	LP	380	(Bourdier 1967; Leonardi 1976)
Vaufrey	France	Europe	Bone	MP-M	120±10	(d'Errico *et al.* 2009; Vincent 1988)
Bilzingsleben	Germany	Europe	Bone	LP	412–320	(Mania & Mania 1988)
Gorham`s Cave	Gibraltar	Europe	Bedrock	MP-M	>39	(Rodríguez-Vidal *et al.* 2014)
Tata	Hungary	Europe	Shell	MP-M	>70	(Marshack 1976; 1990)
Grotta di Fumane	Italy	Europe	Flint; Pebble	MP-M	MIS5,4 & 3	(Leonardi 1981; Peresani *et al.* 2014)
Grotta Maggiore di San Bernardino	Italy	Europe	Flint	MP-M	59–44	(Peresani *et al.* 2014)
Riparo Tagliente	Italy	Europe	Flint; Pebble	MP-M	MIS3	(Leonardi 1983; 1988; Peresani *et al.* 2014)
Pešturina	Serbia	Europe	Bone	MP-Ch/Qt	95–64	(Majkić *et al.* 2018a)
Axlor	Spain	Europe	Pebble	MP	47.5	(García-Diez *et al.* 2013)
Grotta del Cavallo	Spain	Europe	Flint; Slab; Pebble	MP-M	MIS3	(Buggiani *et al.* 2004)
Grotta dell'Alto	Spain	Europe	Pebble	MP-M	MIS3	(Borzatti von Löwenstern & Magaldi 1967)
Kiik-Koba	Ukraine	Europe	Flint	MP-PM	32	(Stepanchuk 2006; Majkić *et al.* 2018b)
Prolom II	Ukraine	Europe	Bone	MP	41–28	(Stepanchuk 1993)
Zaskalnaya V	Ukraine	Europe	Ochre	MP-M	>47	(Stepanchuk 2006)

Material: OES = ostrich egg shell

Cultural attribution: C = Chatelperronian; C&F = Cores and flakes technology; Ch/Qt = Charentian Quina type; ELSA = early Late Stone Age; LM = Late Mousterian; LP = Lower Paleolithic; M = Mousterian; MP = Middle Paleolithic; MSA = Middle Stone Age; PM = para-Micoquian.

OSM 2. Site description.

Lingjing (34° 04' 08.6" north, 113° 40' 47.5" east, elevation 117m) is an open-air site located in northeast Xuchang county, Henan Province, northern China, about 120km south of the Yellow River (Figure 1). The site, a water-lain deposit, was discovered in 1965 when microblades, microcores (Chen 1983), and faunal remains were found on the surface (Li *et al.* 2017b). Since 2005, 551m^2 was excavated under the supervision of one of us (L.Z.). The site features a 9m deep sedimentary sequence comprising eleven geological layers. The sequence includes from the top to the bottom: layers 1-4, Holocene in age, with material culture spanning from the Shang-Zhou Bronze Age to the Neolithic; layer 5 (yellowish silt), LGM to the Younger Dryas, with microblade technology, microcores, bone artefacts, perforated ostrich eggshells, ochre, faunal remains and the first evidence of pottery appearing in the region (Li & Ma 2016; Li *et al.* 2017a); layer 6 (flowstone layer), sterile; layer 7 (yellowish silt), sterile; layer 8 (black ferruginous soil), sterile; layer 9 (brownish ferruginous silt), sterile; layer 10 (brownish ferruginous silt), early Late Pleistocene with lithic artefacts and faunal remains (Li *et al.* 2018); layer 11 (sage-green silt), early Late Pleistocene, with abundant lithic and osseous technologies as well as faunal remains, associated with two incomplete human skulls (Li *et al.* 2017b). The faunal assemblage from this last layer is mostly composed of *Equus caballus*, *Equus hemionus*, and *Bos primigenius* remains. Skeletal elements of *Megaloceros ordosianus*, *Cervus elaphus*, *Coelodonta antiquitatis*, *Procapra przewalskii*, *Dicerorhinus mercki*, *Pachycrocuta* cf. *sinensis*, *Palaeoloxodon* sp., *Viverra* cf. *zibetha*, *Ursus* sp., *Sus lydekkeri*, *Hydropotes pleistocenica*, and *Axis shansius lingjingensis* subsp. nov. were also identified (Li & Dong 2007; Dong & Li 2009). Hyena remains and coprolithes were found at the site (Li & Dong 2007; Wenjuan Wang *et al.* 2014, 2015) but this specie played a marginal role in the accumulation of the faunal assemblage. The high proportion of limb bones (>60 per cent), the high frequency of cut marks (~34 per cent), and their location on the bones suggest that Lingjing layer 11 was a kill-butchery site (Zhang *et al.* 2011, 2012).

OSL ages from layer 11 indicate a deposition taking place at *c.* 125–105 ka BP (Nian *et al.* 2009). This age situates the human occupation during the early phases of MIS5 (MIS5e to MIS5d). The lithic assemblage is mostly composed of quartz and quartzite artefacts, and of sandstone and basalt in marginal proportions (Li *et al.* 2018). The presence of cores, flakes, formal tools (i.e., scrapers, notches, denticulates, borers, points, choppers, etc.), debris, and the identification of use wear on some artefacts suggest that knapping activities, and tool manufacture and use occurred at the site (Li 2007). A few limb bone fragments and an antler bear traces indicating that they were used to retouch stone tools (Doyon *et al.* 2018). The two engraved bone fragments described in this study come from layer 11. They were discovered in 2009 (catalogue numbers 9L0141 and 9L0148) and identified by some of us (L.Z., L.H., L.D., F.D.) as engraved during an analysis of the faunal assemblage conducted in 2016.

OSM 3. Materials and methods

SEM-EDS analysis of the red residue trapped in the lines on specimen 9L0141 was attempted with a JEOL JSM-6700F. Backscattered electron images (BSE) and elemental analyses were conducted under a low vacuum mode with an accelerating voltage of 3kV. BSE images were collected with a SiLi detector and EDS analyses with a SDD-EDAX detector. The analysis was interrupted for conservation before reliable EDS spectra could be acquired owing to the appearance of micro-cracks on the bone surface.

Raman analyses on specimen 9L0141 were conducted with an inVia Qotor confocal Raman Microscope (Renishaw) equipped with an internal calibration system. The analyses were done with a 785nm laser and a power of 0.5 per cent in order to avoid transformation of mineral phases. Acquisition time was set to 10s and multiple co-additions. The spectrometer worked in a spectral range from 100 to 1500cm^{-1}. Five areas were analysed, three with and two without red residue. Data was collected with the software package WIRE3. A sample of haematite curated at the Institute of Cultural Heritage, Shandong University, was also analysed following the same procedure. The mineral phase identification was based on the comparison of the recorded spectra with those of several spectra libraries (de Faria *et al.* 1997; Castro *et al.* 2005).

Sediment trapped in the spongy bone of specimen 9L0141 (OSM 8) was sampled under microscope, and analysed with a JEOL JSM-6460LV SEM. The observations and analyses were conducted under a low vacuum mode by using an accelerating voltage of 20kV. Element analyses were carried out with an EDS INCA Oxford 300 spectrometer. During the analyses, the working distance was kept constant (8mm). Acquisition time was set up to 60 seconds for each EDS spectrum with an average downtime of 40 per cent.

Two sediment samples were collected in 2016 from layer 11, west profile. ED-XRF analysis of these samples was carried out using a portable SPECTRO xSORT X-ray fluorescence spectrometer from AMETEK equipped with a silicon drift detector (SDD) and a low power W X-ray tube with an excitation source of 40kV. Samples were positioned above a 7mm diameter spectrometer aperture and analysed from below for 60 seconds. For data treatment, we used the peak count rates of all detected elements and quantitative data for a selection of elements. The quantitative data were calculated according to a calibration operated with AMETEK X-LabPro software. This calibration was constructed by using 12 certified and local references and allows for the semi-quantification of 7 major and trace elements among the most abundant in ferruginous rocks (normalised concentrations are presented in oxide weight).

OSM 4. Taphonomic analysis.

Table S2. Bone modifications recorded on Lingjing faunal remains analysed in this study.

	n	Non-human			Human			
		Root etching	Carnivore	Digestion	Cutmarks	Marrow extraction	Retouchers	Burnt bone
Total	**227**	**50**	**9**	**5**	**54**	**8**	**7**	**3**
Percentage	**100%**	**22.03%**	**3.96%**	**2.20%**	**23.79%**	**3.52%**	**3.08%**	**1.32%**

Table S3. Data on cut marks identified on Lingjing faunal remains.

Catalogue n°	Number of cut marks	Arrangement	Morphology	Side striations	Changes in direction (*n*)	Edge morphology	Surface breaks (*n*)
7L036	15	Parallel	Straight	Yes	Yes (1)	Clean and Fringed	Yes (3)
6L1019	4	Parallel	Straight	Yes	No	Clean	No
5L004	2	Parallel	Curved	No	No	Clean	No
14L832a	7	Sub-parallel	Straight and Curved	No	No	Clean	No
14L832b	6	Divergent	Straight and Curved	Yes	No	Clean	No
5L858	2	Divergent	Straight and Curved	No	No	Clean	No
14L728	1	na	Straight	Yes	No	Clean	No
15L079	1	na	Straight	No	Yes (1)	Clean	No
6L1415a	6	Overlapping	Straight	Yes	No	Clean	Yes (1)
6L1415b	2	Divergent	Sinuous	No	Yes (2)	Clean	No
10L372	6	Sub-parallel	Straight	Yes	No	Clean	Yes (2)
9L0143	4	Parallel and Divergent	Straight	No	Yes (one has 3)	Clean	No
6L2544	2	Parallel	Sinuous and Curved	Yes	Yes (1)	Clean	No
8L0500	2	Parallel	Straight	No	No	Clean	No
6L2050	8	Divergent	Curved	No	No	Clean	No
14L764	1	na	Sinuous	No	Yes (1)	Clean	No
6L2095	1	na	Straight	No	No	Clean	No
15L077	8	Parallel	Straight	No	No	Clean	No
5L571	2	Parallel	Curved	Yes	No	Clean	No
6L1997	8	Divergent	Straight and Curved	Yes	Yes (1)	Clean	No
6L2197	4	Sub-parallel	Straight and Curved	No	No	Clean	No
9L0094	8	Parallel	Straight	Yes	No	Clean	No
6L780	12	Sub-parallel	Straight	No	Yes (2 due to bone morphology)	Clean	No
6L2034	4	Divergent	Straight	No	Yes (1)	Clean	No
6L771	1	na	Straight	No	No	Clean	No
9L0148	10	Parallel	Straight	No	No	Clean	No

OSM 5. Morphometric and technological data on Lingjing engraved specimens.

Table S4. Morphometric and technological data on specimen 9L0141.

Lines	Start line (before or after fracture)	End line (before or after fracture)	Morphology				Technology				
			Section	Shape	Line keeps a constant depth on concave and convex area	Internal striations	Side striations	Bone breaks	Change in direction	Presence of residue	Same tool
1	na	Before	Asymmetrical to the right	U with flat base	Yes	No	No	Yes (1)	Yes (4)	No	a
2	Before	Before	Asymmetrical to the right	U with flat base	Yes	No	Yes (left [single])	Yes (5)*	Yes (3)	Yes	a
3	na	na	Asymmetrical to the right	U with polygonal base	Yes	Yes	Yes (right [single]; left [single])	Yes (2)	Yes (4)	No	b
4	After	Before	Asymmetrical to the right	U with polygonal base	Yes	Yes	Yes (right [double]; left [single])	Yes (1)	Yes (7)	Yes	b
5	na	na	Asymmetrical to the right	U with flat base	Yes	Yes	Yes (right [double]; left [single])	Yes (1)	Yes (5)	Yes	b
6a	na	na	na	na	Too superficial	na	na	No	No	No	na
6b	na	na	Symmetrical	U	Too superficial	Yes	No	No	Yes (3)	Yes	b
6c	na	na	Asymmetrical to the right	U with polygonal base	Too superficial	Yes	No	No	Yes (2)	Yes	b
7a	na	na	na	na	Too superficial	na	No	No	No	No	na
7b	na	na	Asymmetrical to the right	U with polygonal base	Yes	Yes	No	No	No	No	b
7c	na	na	na	na	Too superficial	na	No	No	No	No	na
7d	na	na	Asymmetrical to the right	U with polygonal base	Yes	Yes	No	No	No	No	b
7e	na	na	na	na	Too superficial	na	No	No	No	No	na

Table S5. Morphometric and technological data on specimen 9L0148.

Lines	Start line (before or after fracture)	End line (before or after fracture)	Morphology		Technology					
			Section	Shape	Internal striations	Side striations	Bone breaks	Change in direction	Presence of residue	Same tool
1	Before	Before	Asymmetrical to the right	Polygonal	Yes	No		No	No	a
2	Before	Before	Asymmetrical to the right	Polygonal	Yes	No		No	No	a
3	Before	na	Asymmetrical to the right	Polygonal	Yes	No		No	No	a
4	Before	na	Asymmetrical to the right	Polygonal	Yes	No		No	No	a
5	Before	Before	Asymmetrical to the right	Polygonal	Yes	No	Yes	No	No	a
6	Before	na	Asymmetrical to the right	Polygonal	Yes	No		No	No	a
7	Before	na	Symmetrical	Polygonal	Yes	No	Yes	No	No	a
8	Before	Before	Symmetrical	Polygonal	Yes	No	Yes	No	No	a
9	Before	na	Symmetrical	Polygonal	Yes	No		No	No	a
10	Before	na	Symmetrical	Polygonal	Yes	No	Yes	No	No	a

OSM 6. Microscopic analysis of specimen 9L0141.

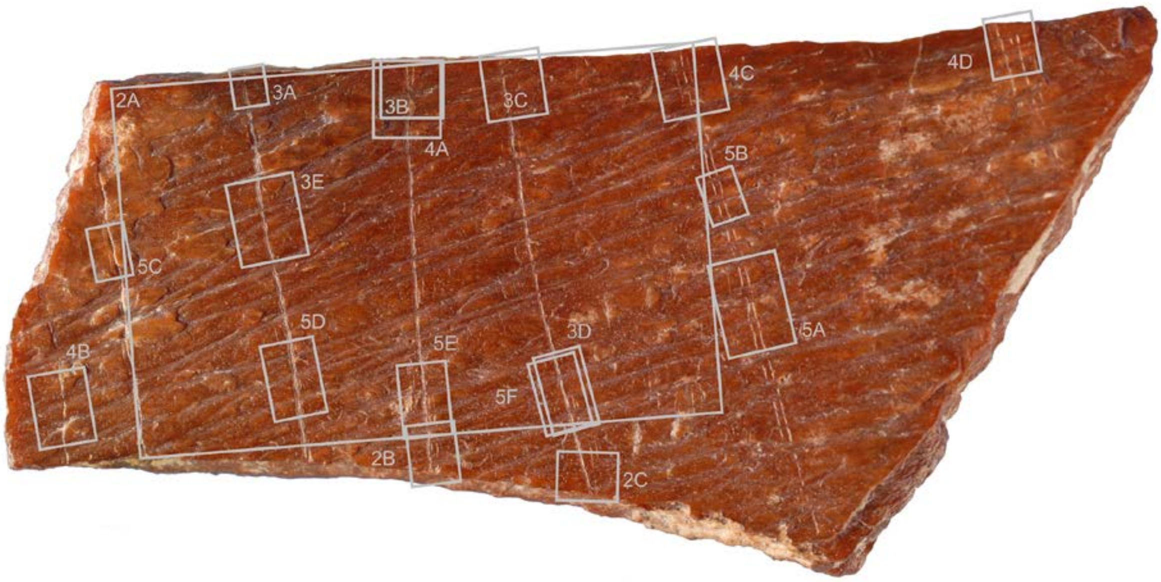

Figure S1. Location of the microscopic photographs present in OSM 6, Figures S2–5.

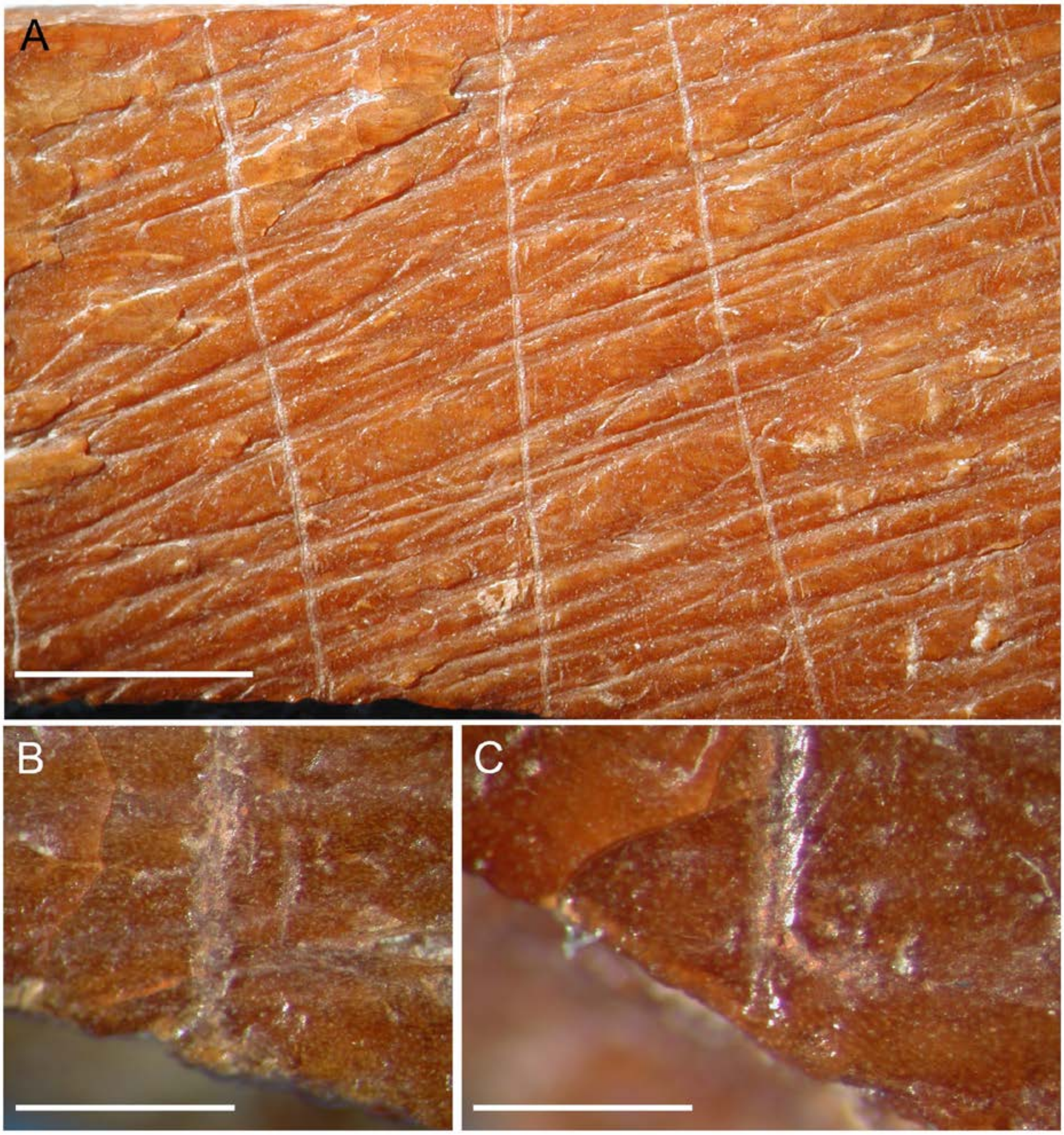

Figure S2. (A) Periosteal surface of specimen 9L0141 showing a rugged fibrous structure. Lower termination of lines (B) L4 and (C) L5 showing that they were interrupted by the fracture of the bone. Scales: A) 5mm; B–C) 500µm.

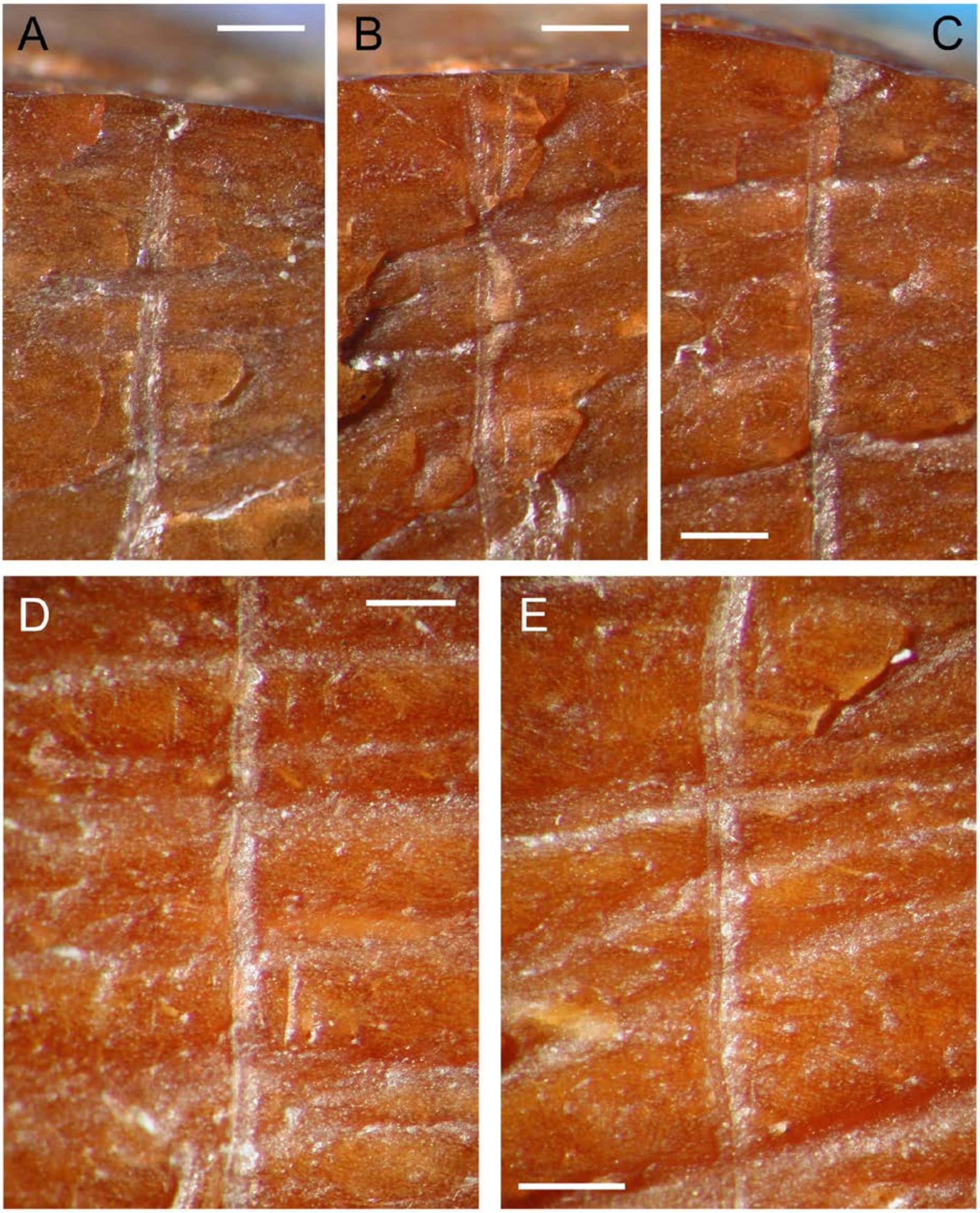

Figure S3. Upper termination of lines (A) L3, (B) L4 and (C) L5, showing that they were engraved after the fracture of the bone. Notice (D) the grainy appearance of the line's surface and (E) the micro-fringed outlines. Scales: A–E) 500µm.

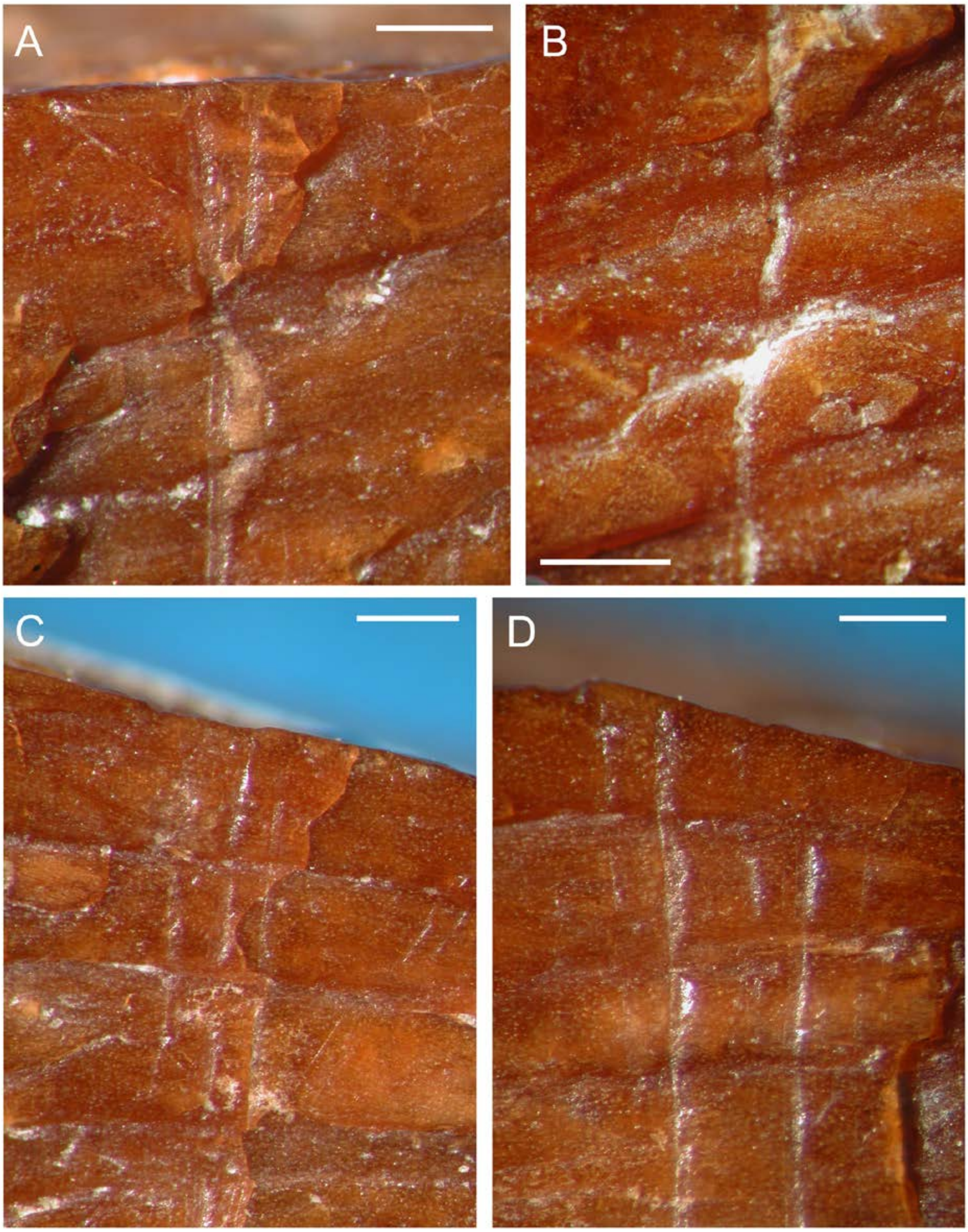

Figure S4. Close-up view of lines (A) L4, (B) L1, (C) L6 and (D) L7. Notice (A) the step micro-fractures occurring when the line crosses natural ridges. (B) Changes in direction of the line and micro-fractures produced when crossing the ridge indicate the direction of the motion. Scales: A–D) 500µm.

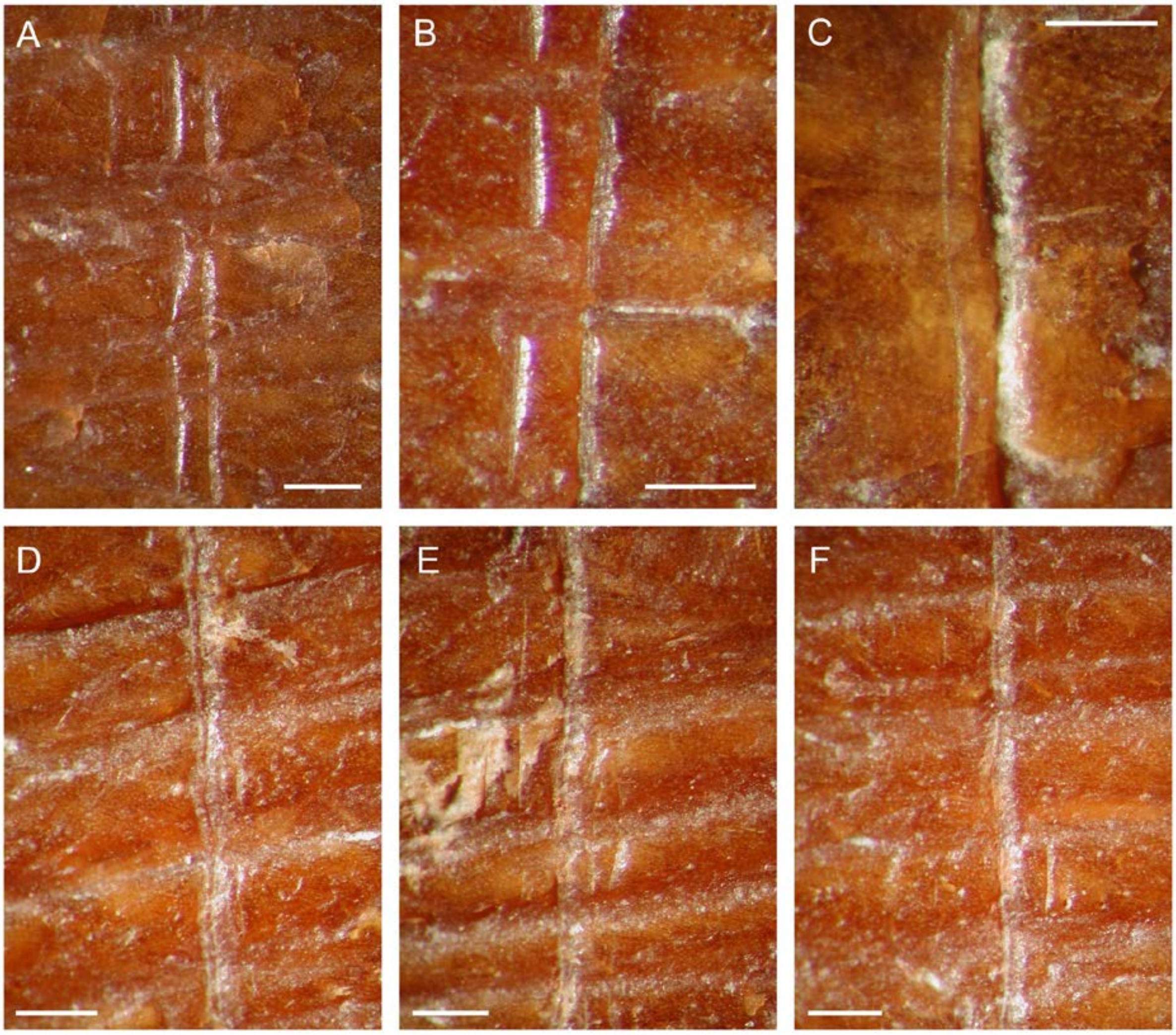

Figure S5. Close-up view of lines (A–B) L6, (C) L2, (D) L3, (E) L4, and (E) L5 on specimen 9L0141. Notice changes in direction (A–B) indicating that the line was engraved my multiple strokes using the same tool (B). Side striations (C–F) result from the discontinuous contact of protuberances on the tool tip. Scales: A–F) 500µm.

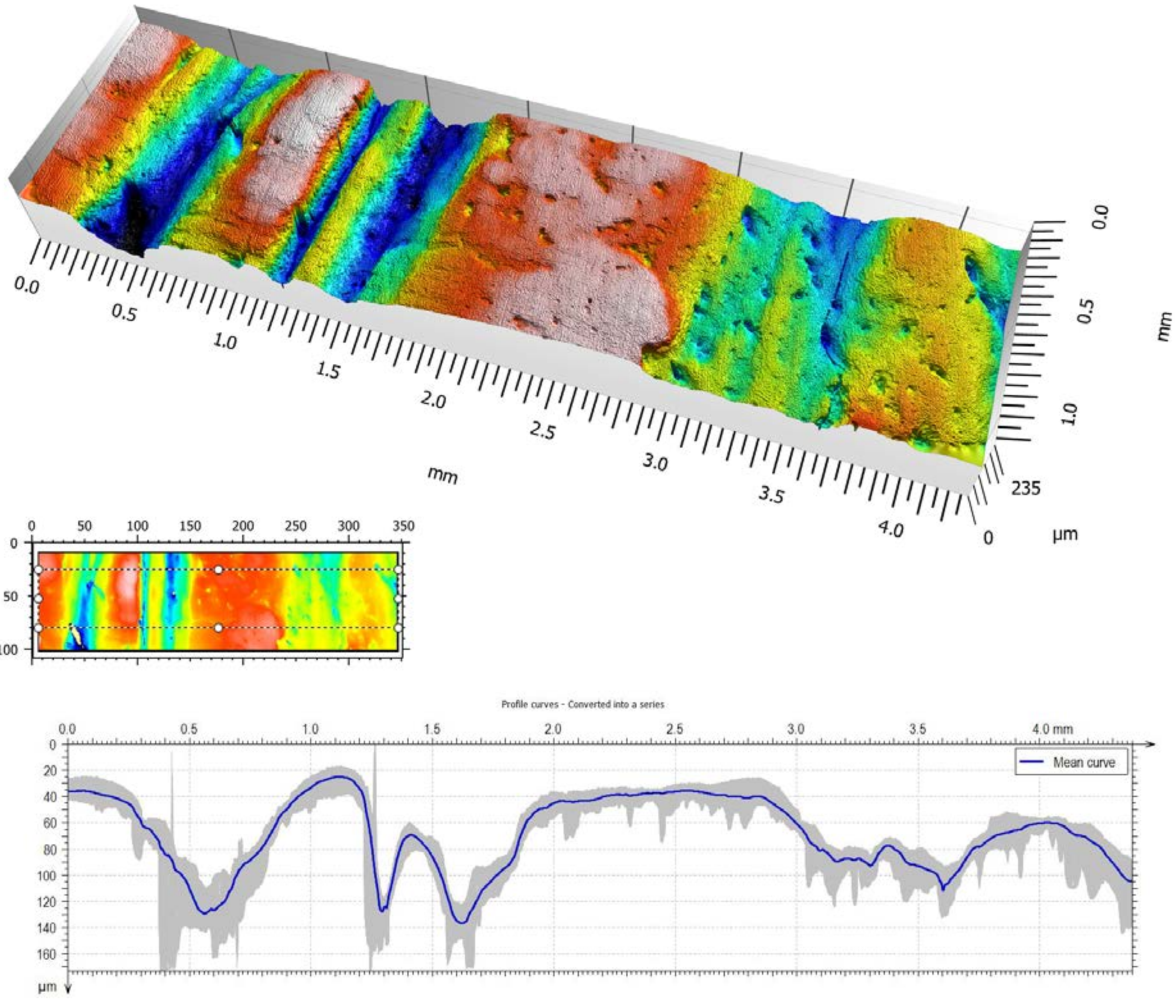

Figure S6. 3D rendering of a selected area of the bone periosteal surface on specimen 9L0141 (top) showing its rugged morphology; (bottom) mean profile curve (blue) of the area indicated in the sketch (centre). Grey surface summarises depth variation.

OSM 7. Residue and sediment analysis.

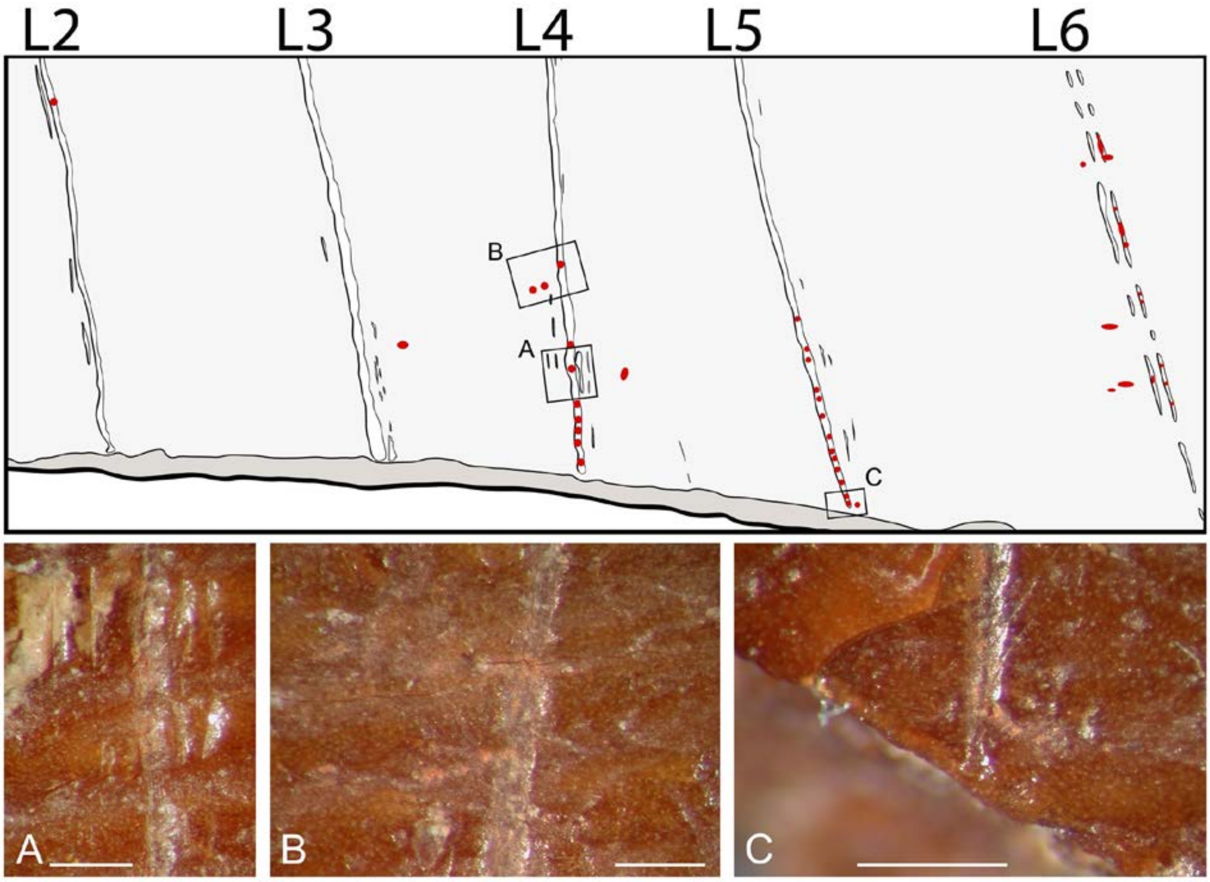

Figure S7. Location of red residues on specimen 9L0141 (top), and close-up view of residues on lines (A–B) L4, (C) L5. Scales: A–C) 500µm.

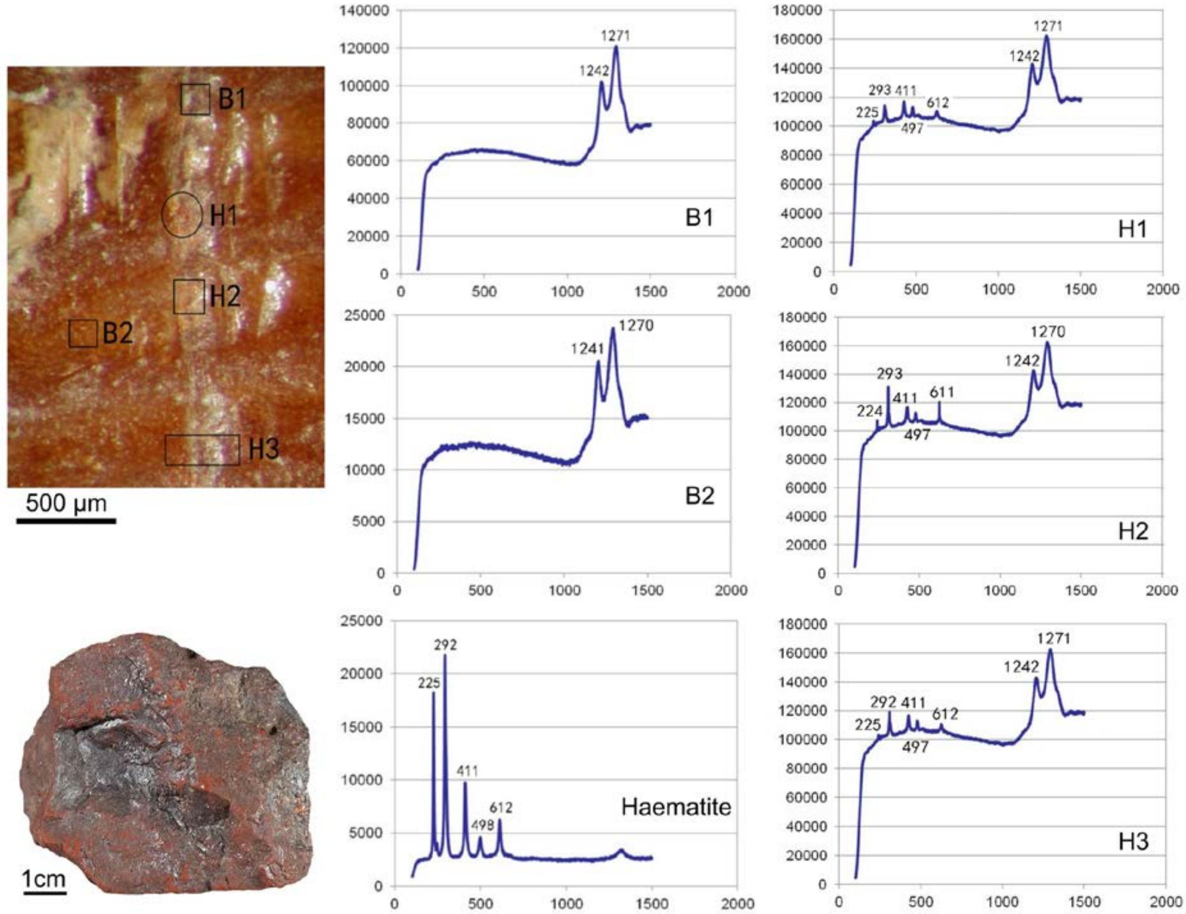

Figure S8. Location of Raman analyses (top left) on specimen 9L0141. B1-B2: bone surface; H1–3: red residues. Haematite fragment curated at the Institute of Cultural Heritage, Shandong University, used for comparison (bottom left), and Raman spectra obtained from analysed spots (right).

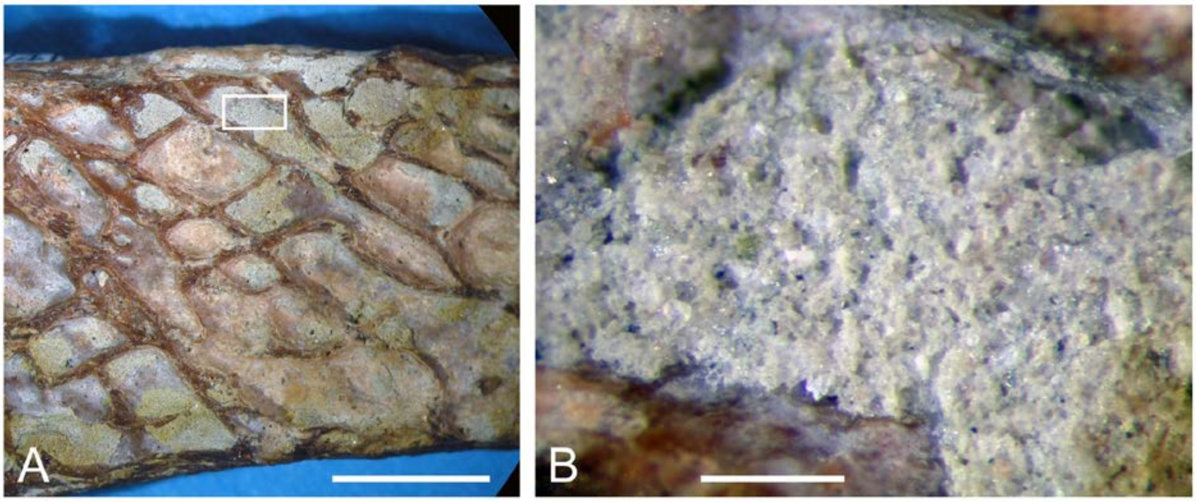

Figure S9. Endosteal surface of specimen 9L0141 with spongy bone (A) filled with sediment (B) from layer 11. Notice the whitish colour of the sediment and the absence of red particles. Scales: A) 5mm; B) 500µm.

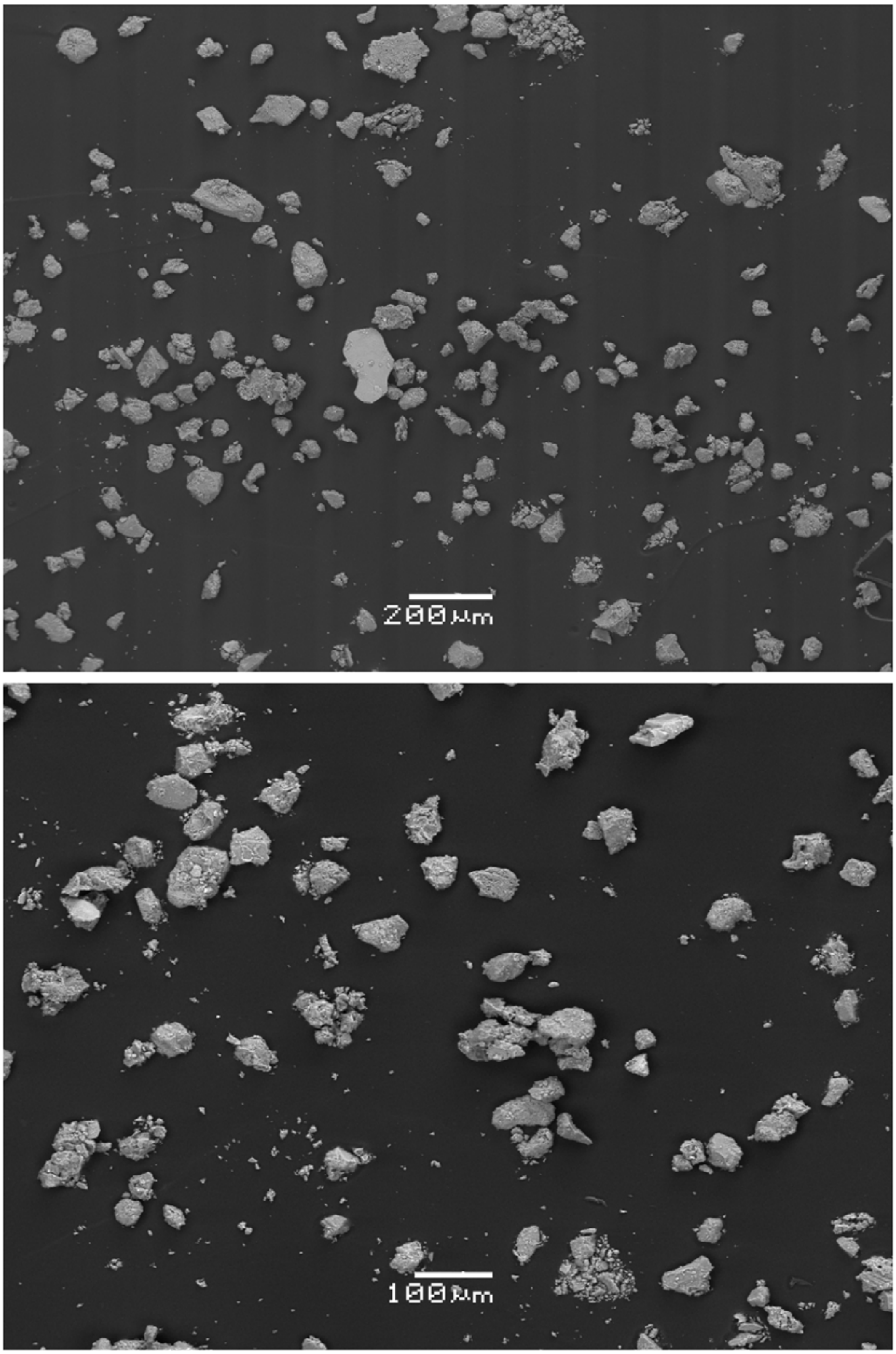

Figure S10. SEM photographs in backscattered mode of particles composing the sediment sampled from the spongy bone of specimen 9L0141.

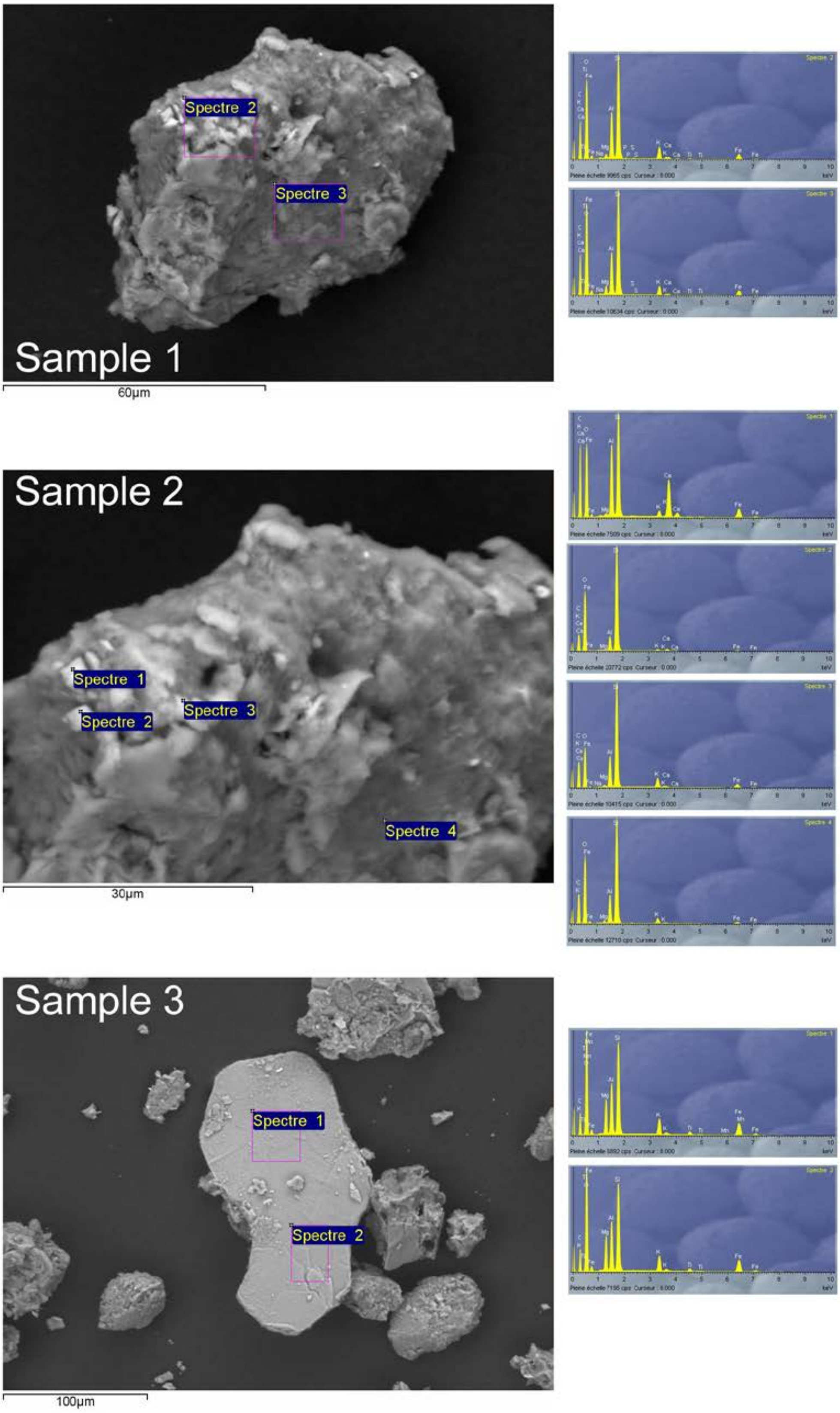

Figure S11. SEM-EDS analyses of sediment particles (samples 1–3) sampled from the spongy bone of specimen 9L0141 (for detailed results, see Table S6).

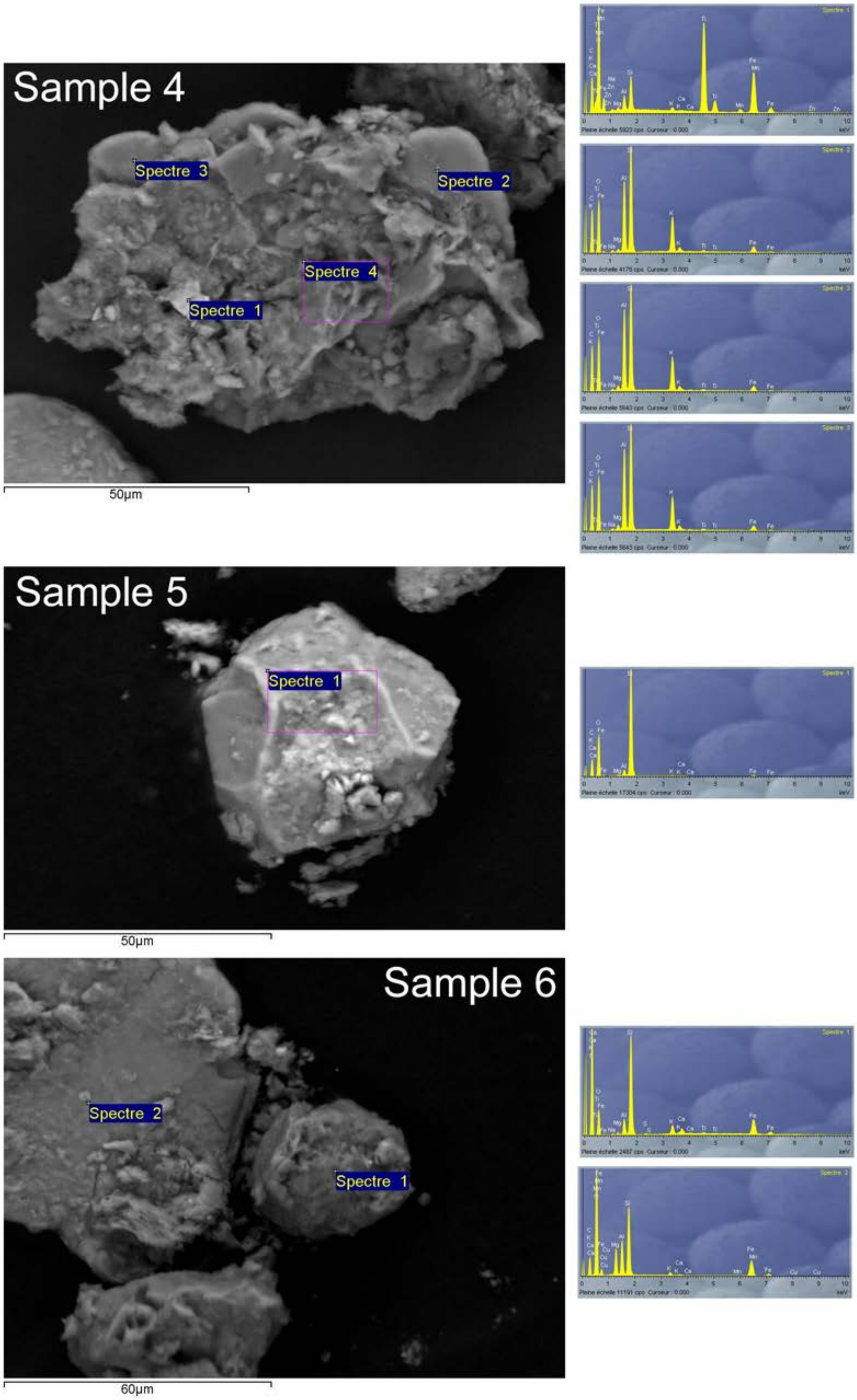

Figure S12. SEM-EDS analyses of sediment particles (samples 4–6) sampled from the spongy bone of specimen 9L0141 (for detailed results, see Table S6).

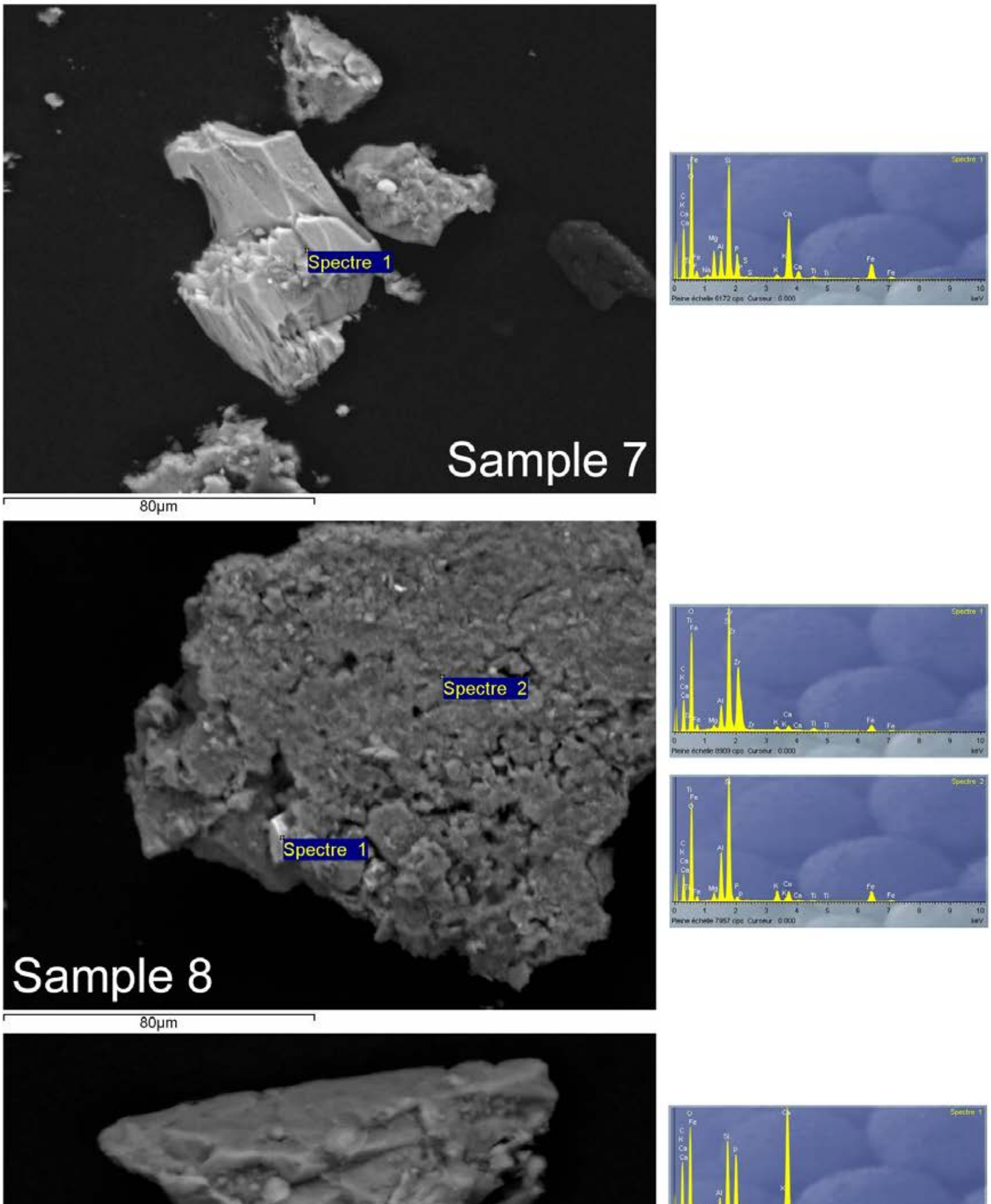

Figure S13. SEM-EDS analyses of sediment particles (samples 7–9) sampled from the spongy bone of specimen 9L0141 (for detailed results, see Table S6).

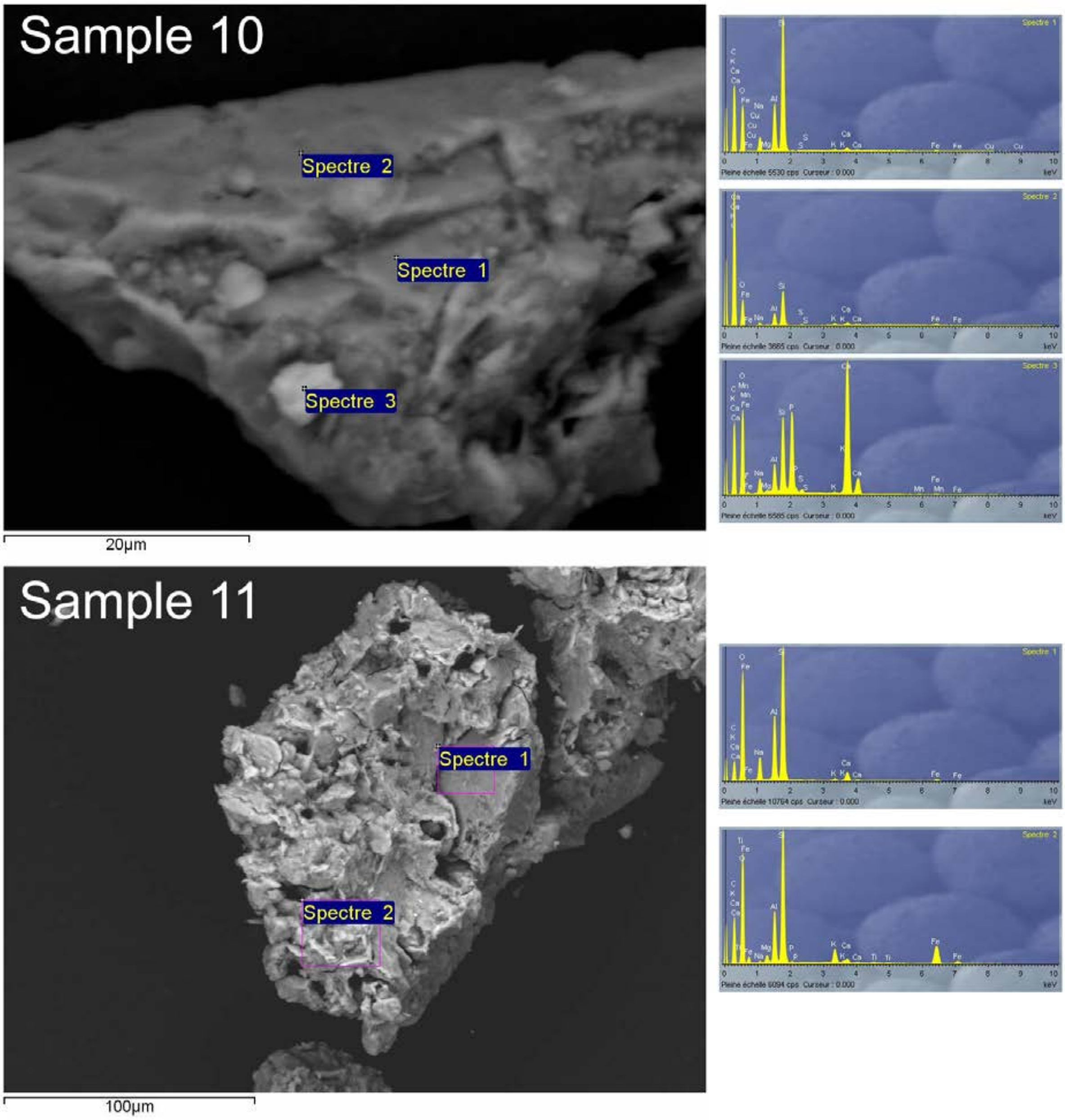

Figure S14. SEM-EDS analyses of sediment particles (samples 10–11) sampled from the spongy bone of specimen 9L0141 (for detailed results, see Table S6).

Table S6. Proportion of chemical elements detected by SEM-EDS on the sediment sampled from the spongy bone of specimen 9L0141 (high content in red).

Sample	Zone	Type	Na_2O	MgO	Al_2O_3	SiO_2	P_2O_5	K_2O	CaO	TiO_2	MnO	Fe_2O_3	CuO	ZnO	ZrO_2	Total
1	2	Clay	0.4	1.9	20.7	58.4	0.5	6.1	1.2	0.6	0.0	10.1	0.0	0.0	0.0	99.9
1	3	Clay	0.3	4.3	19.5	60.5	0.0	4.7	0.6	0.3	0.0	9.3	0.3	0.0	0.0	99.8
2	1	Clay	0.3	0.8	23.6	42.8	0.0	2.4	17.8	0.0	0.0	12.2	0.0	0.0	0.0	99.9
2	2	Clay	0.2	0.6	9.4	83.0	0.0	1.8	2.6	0.0	0.0	2.5	0.0	0.0	0.0	100.0
2	3	Clay	0.3	1.3	16.2	66.5	0.0	5.8	0.5	0.3	0.0	8.6	0.4	0.0	0.0	99.9
2	4	Clay	0.2	1.6	15.8	72.6	0.0	3.9	0.4	0.2	0.0	5.2	0.0	0.0	0.0	99.9
3	1	Clay	0.0	13.5	19.4	41.6	0.0	5.8	0.3	2.5	0.3	16.6	0.0	0.0	0.0	100.0
3	2	Clay	0.0	13.8	19.6	41.1	0.0	5.8	0.3	2.4	0.2	16.8	0.0	0.0	0.0	99.9
4	1	Iron	0.4	0.8	4.0	9.6	0.0	0.8	0.3	45.5	2.2	35.6	0.0	0.9	0.0	100.0
4	2	Clay	0.7	1.0	25.2	48.3	0.0	14.4	0.4	1.4	0.0	8.7	0.0	0.0	0.0	100.0
4	3	Clay	0.5	1.7	28.1	47.9	0.0	13.2	0.4	0.8	0.0	7.3	0.0	0.0	0.0	100.0
4	4	Clay	0.4	3.3	21.9	55.6	0.7	4.9	1.5	1.1	0.0	10.7	0.0	0.0	0.0	99.9
5	1	Quartz	0.2	0.8	4.1	90.3	0.0	0.9	0.3	0.0	0.0	3.4	0.0	0.0	0.0	99.9
6	1	Clay	0.5	1.3	7.6	53.7	0.0	4.3	3.0	0.9	0.0	27.0	1.2	0.0	0.0	99.6
6	2	Clay	0.0	14.1	17.8	40.1	0.0	1.3	0.4	0.0	0.3	25.9	0.3	0.0	0.0	100.0
7	1	Clay	0.7	8.0	7.1	33.4	11.8	1.0	20.5	1.3	0.3	15.7	0.0	0.0	0.0	99.8
8	1	Zircon	0.0	1.4	6.4	35.5	0.0	1.3	1.8	1.7	0.0	7.4	0.0	0.0	44.6	100.0
8	2	Clay	0.2	2.9	17.0	52.8	3.0	3.9	4.7	0.6	0.0	14.9	0.0	0.0	0.0	99.9
9	1	Bone	4.1	0.4	6.8	20.9	28.5	0.3	37.2	0.0	0.3	0.7	0.4	0.0	0.0	99.5
10	1	Clay	6.1	0.3	19.6	69.5	0.0	0.6	2.0	0.0	0.0	1.0	0.7	0.0	0.0	99.8
10	2	Clay	4.6	0.0	17.4	62.3	0.0	3.1	5.3	0.0	0.0	6.1	0.0	0.0	0.0	98.7
10	3	Bone	3.5	0.3	6.0	17.6	30.6	0.3	39.8	0.0	0.4	0.8	0.3	0.0	0.0	99.5
11	1	Clay	8.6	0.2	22.9	60.5	0.0	0.7	4.3	0.0	0.0	2.5	0.3	0.0	0.0	100.0
11	2	Clay	0.6	2.6	16.5	50.8	0.8	4.5	1.7	0.8	0.0	21.7	0.0	0.0	0.0	100.0

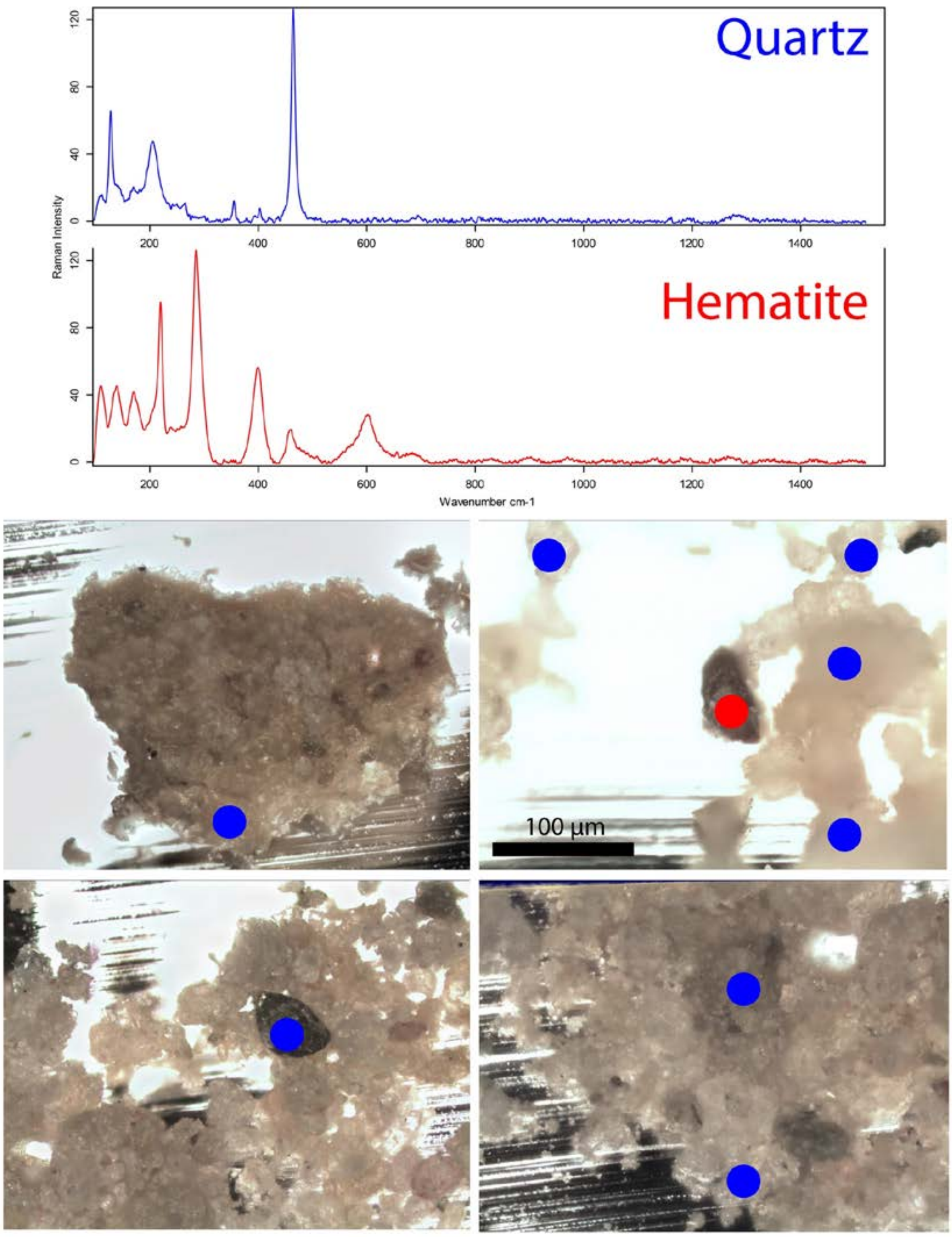

Figure S15. Raman spectra (top) for quartz (blue) and haematite (red) obtained when analysing dark particles in sediment from Lingjing, layer 11 (bottom).

Table S7. Elemental composition of sediment from Lingjing, layer 11 (ED-XRF).

Element	Si	K	Ca	Ti	V	Cr	Mn	Fe	Ni	Zn	Ga	As	Rb	Sr	Y	Zr	Ba	Pb	Th
Dimension	%	%	%	%	µg/g	µg/g	%	%	µg/g	µg/g	µg/g	µg/g	µg/g	µg/g	µg/g	µg/g	µg/g	µg/g	µg/g
Lingjing (Dry Sediment)	33.17	2.007	0.6343	0.3526	< 2,4	41.7	0.05517	2.599	20.1	36.1	14.2	8.4	150.5	135.3	32.9	358.6	555	9.9	11.9
Lingjing (Wet Sediment)	33.19	1.865	0.6206	0.3652	< 2,4	29	0.02451	2.4	19.9	44.4	13.9	10.6	126	170.2	26.8	315.4	515	8.7	7.8

References

BAHN, P.G. & J. VERTUT. 1997. *Journey through the Ice Age*. Los Angeles: University of California Press.

BORZATTI VON LÖWENSTERN, E. & D. MAGALDI. 1967. Ultime ricerche nella Grotta dell'Alto (S. Caterina, Lecce). *Rivista di scienze preistoriche* 22: 205–50.

BOURDIER, F. 1967. *Préhistoire de France*. Paris: Flammarion.

BUGGIANI, S., L. SARTI & F. MARTINI. 2004. Incisioni musteriane su pietra da Grotta del Cavallo (Lecce): contributo al dibattio sulle esperienze grafiche neandertaliane. *Rivista di scienze preistoriche* 54: 271–90.

CAIN, C.R. 2004. Notched, flaked and ground bone artefacts from Middle Stone Age and Iron Age layers of Sibudu Cave, KwaZulu-Natal, South Africa. *South African Journal of Science* 100: 195–97.

CAPITAN, L. & D. PEYRONY. 1912. La station préhistorique de la Ferrassie. *Revue Anthropologique* 22: 76–99.

CASTRO, K., M. PÉREZ-ALONSO, M.D. RODRÍGUEZ-LASO, L.A. FERNÁNDEZ & J.M. MADARIAGA. 2005. On-line FT-Raman and dispersive Raman spectra database of artists' materials (e-VISART database). *Analytical and Bioanalytical Chemistry* 382: 248–58. ttps://doi.org/10.1007/s00216-005-3072-0

CHEN, C. 1983. Preliminary exploration of the typology and technology of microcore in China—also of the culture relationship between Northeast Asia and northwestern North America. *Acta Anthropologica Sinica* 2: 331–46.

CRÉMADES, M., H. LAVILLE, N. SIRAKOV & J. KOZLOWSKI. 1995. Une pierre gravée de 50 000 ans B.P. dans les Balkans. *Paléo* 7: 201–209. https://doi.org/10.3406/pal.1995.1215

D'ERRICO, F., J. ZILHÃO, M. JULIEN, D. BAFFIER & J. PELEGRIN. 1998. Neanderthal acculturation in Western Europe? A critical review of the evidence and its interpretation. *Current Anthropology* 39: 1–44. https://doi.org/10.1086/204689

D'ERRICO, F., M. JULIEN, D. LIOLIOS, M. VANHAEREN & D. BAFFIER. 2003a. Many awls in our argument: bone tool manufacture and use in the Châtelperronian and Aurignacian levels of the Grotte du Renne at Arcy-sur-Cure, in J. Zilhao & F. d'Errico (ed.) *The chronology of the Aurignacian and of the transitional technocomplexes: dating, stratigraphies, cultural implications*: 247–70. Lisbon: Instituto Português de Arqueologia.

D'ERRICO, F., C. HENSHILWOOD, G. LAWSON, M. VANHAEREN, A.-M. TILLIER, M. SORESSI, F. BRESSON, B. MAUREILLE, A. NOWELL, J. LAKARRA, L. BACKWELL & M. JULIEN. 2003b. Archaeological evidence for the emergence of language, symbolism, and music: an alternative multidisciplinary perspective. *Journal of World Prehistory* 17: 1–70. https://doi.org/10.1023/A:1023980201043

D'ERRICO, F., M. VANHAEREN, C.S. HENSHILWOOD, G. LAWSON, B. MAUREILLE, D. GAMBIER, A.-M. TILLIER, M. SORESSI & K.L. VAN NIEKERK. 2009. From the origin of language to the diversification of languages: what can archaeology and palaeoanthropology say?, in F. d'Errico & J.-M. Hombert (ed.) *Becoming eloquent: advances in the emergence of language, human cognition, and modern cultures*: 13–68. Amsterdam: John Benjamins.

D'ERRICO, F., R. GARCÍA MORENO & R.F. RIFKIN. 2012a. Technological, elemental and colorimetric analysis of an engraved ochre fragment from the Middle Stone Age levels of Klasies River Cave 1, South Africa. *Journal of Archaeological Science* 39: 942–52. https://doi.org/10.1016/j.jas.2011.10.032

D'ERRICO, F., L. BACKWELL, P. VILLA, I. DEGANO, J.J. LUCEJKO, M.K. BAMFORD, T.F.G. HIGHAM, M.P. COLOMBINI & P.B. BEAUMONT. 2012b. Early evidence of San material culture represented by organic artifacts from Border Cave, South Africa. *Proceedings of the National Academy of Sciences of the USA* 109: 13214–19. https://doi.org/10.1073/pnas.1204213109

D'ERRICO, F., L. DOYON, I. COLAGÉ, A. QUEFFELEC, E. LE VRAUX, G. GIACOBINI, B. VANDERMEERSCH & B. MAUREILLE. 2018. From number sense to number symbols: an archaeological perspective. *Philosophical Transactions of the Royal Society B* 373: 20160518. https://doi.org/10.1098/rstb.2016.0518

DE FARIA, D.L.A., S. VENÂNCIO SILVA & M.T. DE OLIVEIRA. 1997. Raman microspectroscopy of some iron oxides and oxyhydroxides. *Journal of Raman Spectroscopy* 28: 873–78. https://doi.org/10.1002/(SICI)1097-4555(199711)28:11<873::AID-JRS177>3.0.CO;2-B

DONG, W. & Z. LI. 2009. New cervids (Artiodactyla, Mammalia) from the Late Pleistocene of Lingjing Site in Henan Province, China. *Acta Anthropologica Sinica* 28: 319–26.

DOYON, L., Z. LI, H. LI & F. D'ERRICO. 2018. Discovery of *circa* 115 000-year-old bone retouchers at Lingjing, Henan, China. *PLoS ONE* 13: e0194318. https://doi.org/10.1371/journal.pone.0194318

FRAYER, D.W., J. ORSCHIEDT, J. COOK, M.D. RUSSELL & J. RADOVČIĆ. 2006. Krapina 3: cut marks and ritual behavior? *Periodicum Biologorum* 108: 519–24.

GAO, X., W. HUANG, Z. XU, Z. MA & J.W. OLSEN. 2004. 120–150 ka human tooth and ivory engravings from Xinglongdong Cave, Three Gorges Region, South China *Chinese Science Bulletin* 49: 175–80. https://doi.org/10.1360/03wd0214

GARCÍA-DIEZ, M., B.O. FRAILE & I.B. MAESTU. 2013. Neanderthal graphic behavior: the pecked pebble from Axlor rockshelter (northern Spain). *Journal of Anthropological Research* 69: 397–410. https://doi.org/10.3998/jar.0521004.0069.307

GOREN-INBAR, N. 1990. *Quneitra: a Mousterian site on the Golan Heights. Volume 31*. Qedem: Hebrew University of Jerusalem.

HENSHILWOOD, C.S., F. D'ERRICO & I. WATTS. 2009. Engraved ochres from the Middle Stone Age levels at Blombos Cave, South Africa. *Journal of Human Evolution* 57: 27–47. https://doi.org/10.1016/j.jhevol.2009.01.005

HENSHILWOOD, C.S., F. D'ERRICO, R. YATES, Z. JACOBS, C. TRIBOLO, G.A.T. DULLER, N. MERCIER, J.C. SEALY, H. VALLADAS, I. WATTS & A.G. WINTLE. 2002. Emergence of modern human behavior: Middle Stone Age engravings from South Africa. *Science* 295: 1278–80. https://doi.org/10.1126/science.1067575

HENSHILWOOD, C.S., K.L. VAN NIEKERK, S. WURZ, A. DELAGNES, S.J. ARMITAGE, R.F. RIFKIN, K. DOUZE, P. KEENE, M.M. HAALAND, J. REYNARD, E. DISCAMPS & S.S. MIENIES. 2014. Klipdrift Shelter, southern Cape, South Africa: preliminary report on the Howiesons Poort layers. *Journal of Archaeological Science* 45: 284–303. https://doi.org/10.1016/j.jas.2014.01.033

HODGSKISS, T. 2014. Cognitive requirements for ochre use in the Middle Stone Age at Sibudu, South Africa. *Cambridge Archaeological Journal* 24: 405–28. https://doi.org/10.1017/S0959774314000663

HOVERS, E., B. VANDERMEERSCH & O. BAR-YOSEF. 1997. A Middle Paleolithic engraved artefact from Qafzeh Cave, Israel. *Rock Art Research* 14: 79–87.

JAUBERT, J., F. BIGLARI, V. MOURRE, L. BRUXELLES, J.-G. BORDES, S. SHIDRANG, R. NADERI, M. MASHKOUR, B. MAUREILLE, J.-B. MALLYE & Y. QUINIF. 2009. The Middle Palaeolithic occupation of Mar-Tarik, a new Zagros Mousterian site in Bisotun massif (Kermanshah, Iran), in M. Otte, F. Biglari & J. Jaubert (ed.) *Iran Palaeolithic Le paléolithique d'Iran* (British Archaeological Reports International series 1968): 7–27. Oxford: Archaeopress.

JOORDENS, J.C.A. *et al*. 2015. *Homo erectus* at Trinil on Java used shells for tool production and engraving. *Nature* 518: 228–31. https://doi.org/10.1038/nature13962

LANGLEY, M.C., C. CLARKSON & S. ULM. 2008. Behavioural complexity in Eurasian Neanderthal populations: a chronological examination of the archaeological evidence. *Cambridge Archaeological Journal* 18: 289–307. https://doi.org/10.1017/S0959774308000371

LEONARDI, P. 1976. Les incisions pré-leptolithiques du Riparo Tagliente (Verone) et de Terra Amata (Nice) en relation au problème de la naissance de l'art. *Atti della Accademia Nazionale dei Lincei* 8: 35–104.
– 1981. Raschiatoio musteriano del Riparo Solinas di Fumane (Verona) con incisioni sul cortice. *Atti dell'Accademia Roveretana degli Agiati Contributi della Classe di Scienze Umane, Lettere e Arti* 20: 87–92.
– 1983. Incisioni e segni vari paleolitici del Riparo Tagliente di Stallavena nei Monti Lessini presso Verona (Italia). Campagne di scavo 1972–1982. *Atti del Museo Civico di Storia Naturale di Trieste* 34: 143–76.
– 1988. Art paléolithique mobilier et pariétal en Italie. *L'Anthropologie* 92: 139–202.
L'HOMME, V. & E. NORMAND. 1993. Présentation des galets striés de la couche inférieure du gisement moustérien de 'Chez Pourré-Chez Comte' (Corrèze). *Paléo* 5: 121–25. ttps://doi.org/10.3406/pal.1993.1107
LI, H., Z. LI, M.G. LOTTER & K. KUMAN. 2018. Formation processes at the early Late Pleistocene archaic human site of Lingjing, China. *Journal of Archaeological Science* 96: 73-84. https://doi.org/10.1016/j.jas.2018.05.004
LI, Z. 2007. A primary study on the stone artifacts of Lingjing site excavated in 2005. *Acta Anthropologica Sinica* 26: 138–54.
LI, Z. & W. DONG. 2007. Mammalian fauna from the Lingjing Paleolithic site in Xuchang, Henan Province. *Acta Anthropologica Sinica* 26: 345–60.
LI, Z. & H. MA. 2016. Techno-typological analysis of the microlithic assemblage at the Xuchang Man site, Lingjing, central China. *Quaternary International* 400: 120–29. ttps://doi.org/10.1016/j.quaint.2015.08.065
LI, Z., D. KUNIKITA & S. KATO. 2017a. Early pottery from the Lingjing site and the emergence of pottery in northern China. *Quaternary International* 441: 49–61. https://doi.org/10.1016/j.quaint.2016.06.017
LI, Z., X. WU, L. ZHOU, W. LIU, X. GAO, X. NIAN & E. TRINKAUS. 2017b. Late Pleistocene archaic human crania from Xuchang, China. *Science* 355: 969–72. https://doi.org/10.1126/science.aal2482
MACKAY, A. & A. WELZ. 2008. Engraved ochre from a Middle Stone Age context at Klein Kliphuis in the Western Cape of South Africa. *Journal of Archaeological Science* 35: 1521–32. https://doi.org/10.1016/j.jas.2007.10.015
MAJKIĆ, A., F. D'ERRICO, S. MILOŠEVIĆ, D. MIHAILOVIĆ & V. DIMITRIJEVIĆ. 2018a. Sequential incisions on a cave bear bone from the Middle Paleolithic of Pešturina Cave,

Serbia. *Journal of Archaeological Method and Theory* 25: 69–116. https://doi.org/10.1007/s10816-017-9331-5

MAJKIĆ, A., F. D'ERRICO & V. STEPANCHUK. 2018b. Assessing the significance of Palaeolithic engraved cortexes: a case study from the Mousterian site of Kiik-Koba, Crimea. *PLoS ONE* 13: e0195049. https://doi.org/10.1371/journal.pone.0195049

MANIA, D. & U. MANIA. 1988. Deliberate engravings on bone artefacts of *Homo erectus*. *Rock Art Research* 5: 91–95.

MARSHACK, A. 1976. Some implications of the Paleolithic symbolic evidence for the origin of language. *Origins and Evolution of Language and Speech* 280: 289–311.

– 1990. Early hominid symbol and evolution of the human capacity, in P.A. Mellars (ed.) *The emergence of modern humans: and archaeological perspective*: 457–98. Ithaca (NY): Cornell University Press.

MAUREILLE, B. *et al*. 2010. Les Pradelles à Marillac-le-Franc (Charente). Fouilles 2001–2007: nouveaux résultats et synthèse, in J. Buisson-Catil & J. Primault (ed.) *Préhistoire entre Vienne et Charente. Hommes et sociétés du Paléolithique. Association des publications chauvinoises, Mém. XXXVIII*: 145–162. Chauvigny: APC.

NIAN, X.M., L.P. ZHOU & J.T. QIN. 2009. Comparisons of equivalent dose values obtained with different protocols using a lacustrine sediment sample from Xuchang, China. *Radiation Measurements* 44: 512–16. https://doi.org/10.1016/j.radmeas.2009.06.002

PENG, F., X. GAO, H. WANG, F. CHEN, D. LIU & S. PEI. 2012. An engraved artifact from Shuidonggou, an early Late Paleolithic site in Northwest China. *Chinese Science Bulletin* 57: 4594–99. https://doi.org/10.1007/s11434-012-5317-6

PERESANI, M., S. DALLATORRE, P. ASTUTI, M.C. DAL, S. ZIGGIOTTI & C. PERETTO. 2014. Symbolic or utilitarian? Juggling interpretations of Neanderthal behavior: new inferences from the study of engraved stone surfaces. *Journal of Anthropological Sciences* 92: 233–55.

RODRÍGUEZ-VIDAL, J. *et al*. 2014. A rock engraving made by Neanderthals in Gibraltar. *Proceedings of the National Academy of Sciences of the USA* 111: 13301–306. https://doi.org/10.1073/pnas.1411529111

SIRAKOV, N. *et al.* 2010. An ancient continuous human presence in the Balkans and the beginnings of human settlement in Western Eurasia: a Lower Pleistocene example of the Lower Palaeolithic levels in Kozarnika Cave (north-western Bulgaria). *Quaternary International* 223–224: 94–106. https://doi.org/10.1016/j.quaint.2010.02.023

STEPANCHUK, V.N. 1993. Prolom II, a Middle Palaeolithic cave site in the Eastern Crimea with non-utilitarian bone artefacts. *Proceedings of the Prehistoric Society* 59: 17–37. https://doi.org/10.1017/S0079497X0000373X

– 2006. *The Lower and Middle Paleolithic of Ukraine*. Chernovtsy: Zelena Bukovina.

TEXIER, P.-J., G. PORRAZ, J. PARKINGTON, J.-P. RIGAUD, C. POGGENPOEL, C. MILLER, C. TRIBOLO, C. CARTWRIGHT, A. COUDENNEAU, R. KLEIN, T. STEELE & C. VERNA. 2010. A Howiesons Poort tradition of engraving ostrich eggshell containers dated to 60,000 years ago at Diepkloof Rock Shelter, South Africa. *Proceedings of the National Academy of Sciences of the USA* 107: 6180–85. https://doi.org/10.1073/pnas.0913047107

VINCENT, A. 1988. L'os comme artefact au Paléolithique moyen: principes d'étude et premiers résultats, in M. Otte, L. Binford & J.P. Rigaud (ed.) *L'homme de Néandertal 4, la technique*: 185–96. Liège: ERAUL.

VOGELSANG, R., J. RICHTER, Z. JACOBS, B. EICHHORN, V. LINSEELE & R.G. ROBERTS. 2010. New excavations of Middle Stone Age deposits at Apollo 11 rockshelter, Namibia: stratigraphy, archaeology, chronology and past environments. *Journal of African Archaeology* 8: 185–218. https://doi.org/10.3213/1612-1651-10170

WANG, W., Z. LI, G. SONG & Y. WU. 2015. A study of possible Hyaena coprolites from the Lingjing Site, central China. *Acta Anthropologica Sinica* 34: 117–25.

WANG, W., Y. WU, G. SONG, K. ZHAO & Z. LI. 2014. Pollen and fungi spore analysis on Hyaenid coprolite from the Xuchang Man Site, central China. *Chinese Science Bulletin* 58: 51–56.

WATTS, I. 2010. The pigments from Pinnacle Point Cave 13B, Western Cape, South Africa. *Journal of Human Evolution* 59: 392–411. https://doi.org/10.1016/j.jhevol.2010.07.006

ZHANG, S., X. GAO, Y. ZHANG & Z. LI. 2011. Taphonomic analysis of the Lingjing fauna and the first report of a Middle Paleolithic kill-butchery site in north China. *Chinese Science Bulletin* 56: 3213–19. https://doi.org/10.1007/s11434-011-4718-2

ZHANG, S., Z. LI, Y. ZHANG & X. GAO. 2012. Skeletal element distributions of the large herbivores from the Lingjing site, Henan Province, China. *Science China: Earth Sciences* 55: 246–53. https://doi.org/10.1007/s11430-011-4279-x

ZILHÃO, J. 2007. The emergence of ornaments and art: an archaeological perspective on the origins of 'behavioral modernity'. *Journal of Archaeological Research* 15: 1–54. https://doi.org/10.1007/s10814-006-9008-1